

Rare region effects in the contact process on networks

Róbert Juhász

*Institute for Solid State Physics and Optics,
Wigner Research Centre for Physics,
H-1525 Budapest, P.O.Box 49, Hungary*

Géza Ódor

*Research Centre for Natural Sciences, Hungarian Academy of Sciences,
MTA TTK MFA, H-1525 Budapest, P.O.Box 49, Hungary*

Claudio Castellano

*Istituto dei Sistemi Complessi (ISC-CNR), Via dei Taurini 19, I-00185 Roma, Italy, and
Dipartimento di Fisica, “Sapienza” Università di Roma, P.le A. Moro 2, I-00185 Roma, Italy*

Miguel A. Muñoz

*Departamento de Electromagnetismo y Física de la Materia and Instituto
Carlos I de Física Teórica y Computacional Carlos I. Facultad de Ciencias,
Universidad de Granada, E-18071 Granada, Spain*

(Dated: June 18, 2018)

Networks and dynamical processes occurring on them have become a paradigmatic representation of complex systems. Studying the role of quenched disorder, both intrinsic to nodes and topological, is a key challenge. With this in mind, here we analyze the contact process, i.e. the simplest model for propagation phenomena, with node-dependent infection rates (i.e. intrinsic quenched disorder) on complex networks. We find Griffiths phases and other rare region effects, leading rather generically to anomalously slow (algebraic, logarithmic, etc.) relaxation, on Erdős-Rényi networks. We predict similar effects to exist for other topologies as long as a non-vanishing percolation threshold exists. More strikingly, we find that Griffiths phases can also emerge –even with constant epidemic rates– as a consequence of mere topological heterogeneity. In particular, we find Griffiths phases in finite dimensional networks as, for instance, a family of generalized small-world networks. These results have a broad spectrum of implications for propagation phenomena and other dynamical processes on networks, and are relevant for the analysis of both models and empirical data.

I. INTRODUCTION

Complex networks constitute a useful unifying concept with many interdisciplinary realizations ranging from the World Wide Web and other technological or infrastructure networks to genetic, metabolic, ecological, or social networks [1]. Many efforts have been devoted to elucidate non-trivial topological traits of network architectures; in particular, networks with scale-free and/or small-world properties received a vast amount of attention. In recent years, the research focus shifted to dynamical processes occurring on them [2–4]. Particularly interesting are spreading or transport processes which represent a vast variety of propagation phenomena occurring on networks: microbial epidemics, computer viruses, rumor spreading, or signal propagation in neural nets are some examples.

As it is well-known in Statistical Physics, the presence of *quenched disorder* usually affects the universal behavior of phase transitions. Quenched disorder may also generate novel phases unheard-of in pure systems (both in equilibrium and non-equilibrium situations), as is the case of Griffiths phases (GP). These are extended regions appearing within the disordered phase and characterized –among some other prominent features– by generic anomalously slow dynamics and logarithmic or *activated*

scaling at the transition point [5–8]. These effects stem from the fact that different *rare regions*, which can be in the ordered phase even if the system is globally disordered, emerge in such systems. These regions have a broad distribution of relaxation times and the convolution of them gives rise generically to slow dynamics.

Heterogeneity in the intrinsic properties of nodes, i.e. *quenched disorder*, is a natural feature of real networks: node-dependent rates appear in all the examples of spreading above (owing to the specificity of the individual immune response, presence of anti-virus software, and so forth). Networks with node-dependent intrinsic properties (or “fitnesses”) have been previously studied in the literature [9], but not from the point of view that interests us here. Apart from intrinsic node-disorder, networks have a structural or *topological disorder*, since nodes are in general topologically not equivalent. One can then wonder whether topological disorder by itself may induce Griffith phases or similar rare-regions effects.

The role of intrinsic and topological disorder on the overall properties of dynamical processes taking place on networks has not been much studied so far. In which ways can the node-to-node variability affect the overall probability of epidemics to propagate or to become extinct? Does disorder in the topology of the network modify the basic phenomenology of epidemics? Can novel

phases or new qualitative behaviors appear?

In this paper we tackle the study of quenched disorder –both intrinsic and topological– in dynamical processes on complex networks. For this, we look for rare-region effects in the simplest possible epidemic model, i.e. the contact process [10]. By using different types of disorder and various network topologies we report on the existence of Griffiths effects, including various non-trivial regimes with generic slow decay of activity. In particular, we first study a contact process with node-dependent rates on Erdős-Rényi networks [11] and find strong rare-region effects below the percolation threshold. Then we study a contact process with constant rates but in disordered topologies: we also report on the existence of strong rare region effects in cases in which the underlying topology has a finite topological dimension. Our conclusions are expected to go beyond the specific examples under consideration, and to apply to different models, dynamics and topologies, obeying some minimal requirements. We believe that the non-trivial effects of disorder uncovered here can shed light on anomalous effects observed in many different dynamical problems on networks.

The paper is organized as follows: In Section II we first define the models under investigation, the pure contact process and the disordered quenched contact process. We present a theoretical analysis of the behavior of the latter on networks, based on optimal fluctuations arguments, and compare it with the results of numerical simulations. In Section III we introduce the Generalized Small-World (GSW) networks and the 3-regular random networks and illustrate the results of numerical simulations of the contact process on such topologies. Concluding remarks are in Sec. IV. A preliminary account of this work has been published in Ref. [12].

II. QUENCHED CONTACT PROCESS ON ERDŐS-RÉNYI AND SCALE-FREE NETWORKS

A. Contact Process on networks

Let us consider the pure contact process (CP) [10, 13] defined on a generic topology. Each node can be in one of two states, either infected (active/1) or healthy (inactive/0). An infected node heals at rate μ and, with rate λ , it infects a randomly selected neighbor. If the selected neighbor is already infected nothing happens. In the following μ will be fixed to 1, with no loss of generality.

A zero-th order homogeneous mean-field equation for the average activity density,

$$\dot{\rho}(t) = -\rho(t) + \lambda\rho(t)(1 - \rho(t)), \quad (1)$$

predicts an absorbing phase transition where the infection and healing rates compensate each other: i.e.

$\lambda_c^{(1)} = 1$, and a decay $\rho(t) \sim t^{-1}$ at criticality. A slightly more refined calculation (heterogeneous mean-field approach [14]) takes into account the fact that the average activity density ρ_k depends on the number of connections k (degree) of the corresponding vertex. This again predicts a transition at $\lambda_c^{(1)} = 1$ if the underlying network is uncorrelated (i.e. vanishing degree-degree correlations). These results are expected to be exact for infinite dimensional lattices as well as for fully connected networks. Instead for *finitely connected* networks the threshold is shifted to $\lambda_c > 1$ (as shown in simulations below). This occurs because when activity is low it appears in localized regions, and this decreases the effective rate of infection (i.e. the probability to choose an occupied nearest neighbor is larger than for random mixing). This effect can be taken into account by using a *pair-approximation* (as described in Appendix A). In the case of a regular graph (with all vertices having degree k) it yields an improved estimate of the critical point

$$\lambda_c^{(2)} = \frac{k}{k-1}. \quad (2)$$

Observe that $\lambda_c^{(2)}$ converges to $\lambda_c^{(1)} = 1$ when $k \rightarrow \infty$ (i.e. for infinite connectivity, for which simple mean-field holds) and diverges at the percolation threshold $k = 1$ below which the network becomes fragmented [2, 15, 16] and, consequently, activity cannot be sustained and the phase transition disappears. If the network under consideration is not regular but has some nontrivial degree distribution $P(k)$ it is reasonable to expect that the expression

$$\lambda_c^{(2)} = \frac{\langle k \rangle}{\langle k \rangle - 1}, \quad (3)$$

where $\langle k \rangle$ is the average network connectivity, gives a good approximation for the threshold, provided the network is not very heterogeneous (i.e. that $P(k)$ is narrow). In the case considered in our numerical studies below, $\langle k \rangle = 3$ and, hence, the critical point for the pure CP is predicted to be around $\lambda_c^{(2)} = 3/2$, in rather good agreement with numerical results.

B. Quenched Contact Process on networks

We now consider the Quenched Contact Process (QCP) [7], i. e. a Contact Process with quenched disordered infection rate: a fraction $1 - q$ of the nodes (type-I) take a value λ and the remaining fraction q (type-II nodes) take a reduced value $r\lambda$, with $0 \leq r < 1$:

$$P(\lambda_i) = (1 - q)\delta(\lambda_i - \lambda) + q\delta(\lambda_i - r\lambda) . \quad (4)$$

Obviously, for $q = 0$ and $q = 1$ the model is non-disordered with $\lambda_c(q = 1) = \lambda_c(q = 0)/r$, while for $0 < q < 1$ one expects λ_c to interpolate between these limits. In the general disordered case the density can be

expressed as $\rho = (1 - q)\rho_1 + q\rho_2$, where the sub-index refers to the node type and ρ_i are the corresponding densities. At the homogeneous mean-field level,

$$\dot{\rho}_i(t) = -\rho_i + (1 - \rho_i)[\lambda(1 - q)\rho_1 + r\lambda q\rho_2] \quad (5)$$

for $i = 1, 2$. A standard linear stability analysis leads to, $\lambda_c^1(q) = 1 - q(1 - r)^{-1}$. As in the pure case, this zero-th order result, multiplied by the factor $\langle k \rangle / (\langle k \rangle - 1)$ to account for correlations, provides a good estimate for the threshold in generic networks with narrow degree distribution

$$\lambda_c^{(2)} = \frac{\langle k \rangle}{\langle k \rangle - 1} \frac{1}{1 - q(1 - r)}. \quad (6)$$

Observe that type-I sites exhibit a percolation transition where their intrinsic connectivity, $(1 - q)\langle k \rangle = 1$ [2, 15], i.e. at $q_{perc} = 1 - \langle k \rangle^{-1}$. For larger values of q the network cannot sustain activity if $r = 0$: type-I clusters are finite and type-II ones do not propagate activity. Hence, for $r = 0$, Eq.(6) is valid only for $q < q_{perc}$, while for $r > 0$ it holds generically.

C. Understanding the QCP behavior on Erdős-Rényi networks

The behavior of the QCP model on Erdős-Rényi (ER) random networks [11] can be predicted by using, as often done in disordered systems (see [6-8, 17]), *optimal fluctuation arguments*. These allow to derive the phase-diagram depending on the value of the spreading rate λ and of the fraction q of nodes with reduced infection rate, $r\lambda$ (see Fig. 1 for $r = 0$ and Fig. 4 for $r > 0$).

In what follows, the theoretical predictions for different phases are presented and checked against the results of numerical simulations of the QCP on ER networks with $\langle k \rangle = 3$ (implying $q_{perc} = 2/3$), and sizes up to $N = 10^7$. Simulations are performed in the standard way [18, 19]: a list of type-I and type-II occupied nodes is kept and the total rates r_I and r_{II} are calculated. At each time step with probability $r_j / (r_I + r_{II})$ a site of type j is randomly selected and it either heals (with probability $1 / (1 + \lambda_j)$) or infects a single randomly selected neighbor provided it was empty (with probability $\lambda_j / (1 + \lambda_j)$). Time is increased by $1 / (r_I + r_{II})$ and the procedure is iterated. All sites are active initially and the global density of active nodes $\rho(t)$, averaged over many runs, is monitored.

The basic idea of the optimal fluctuation analysis is that the long-time decay of $\rho(t)$ is controlled by the convolution of different rare regions of type-I sites with different relaxation time. The overall decay can be written as the following convolution integral

$$\rho(t) \sim \int ds s P(s) \exp[-t/\tau(s)] \quad (7)$$

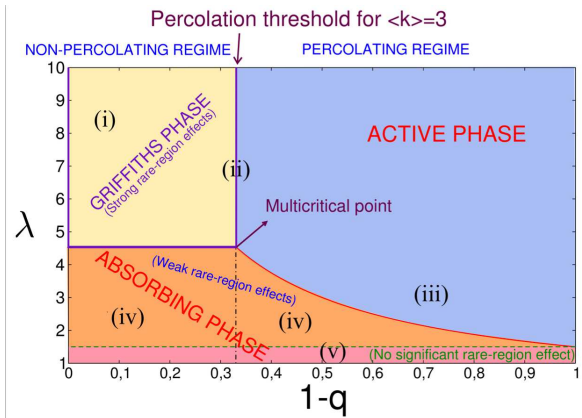


FIG. 1. (Color online) Phase diagram for $\langle k \rangle = 3$ and $r = 0$ as a function of the spreading rate λ and of the fraction of type-I nodes, $1 - q$. See main text for a detailed description of the different phases.

where $P(s)$ is the probability of having a rare region of size s and $\tau(s)$ is the decay time of activity in such a region.

1. Case $r = 0$

We start considering the case $r = 0$. Based on the different possible functional forms of $P(s)$ and the cluster density-decay function in the various regions of the phase-diagram the following regimes can be predicted (see Fig.1):

(i) *Griffiths phase*: $\lambda > \lambda_c(q_{perc})$ and $q > q_{perc}$. For $q > q_{perc}$ the network of type-I nodes is fragmented and consist of finite clusters, whose size distribution is given by [20]:

$$P(s) \sim \frac{1}{\sqrt{2\pi p}} s^{-3/2} e^{-s(p-1-\ln(p))} \quad (8)$$

where p is the average number of links per node, which in our case is $p = \langle k \rangle_{q=0}(1 - q)$ for type-I nodes. Within any given connected cluster of type-I nodes, let us define p_{loc} as the local average number of links per node, and –from it– an effective local value of q , $q_{loc} = 1 - p_{loc} / \langle k \rangle_{q=0}$. Obviously, for connected type-I clusters, $q_{loc} < q_{perc}$, i.e. they are locally above the percolation threshold and hence, provided that $\lambda > \lambda_c(q_{perc})$, they are active rare regions, where activity survives until a coherent random fluctuation extinguishes it. The characteristic decay time $\tau(s)$ grows exponentially (Arrhenius law) with cluster size, i.e. $\tau(s) \simeq t_0 \exp(A(\lambda)s)$, where t_0 and $A(\lambda)$ do not depend on s . Plugging Eq. (8) into Eq. (7) and using a saddle-point approximation, one obtains $\rho(t) \sim t^{-\theta(p,\lambda)}$, with $\theta(p,\lambda) = -(p - 1 - \ln(p)) / A(\lambda)$; i.e. there is a **generic power-law decay with continuously varying exponents**, that is, a Griffiths phase, emerging as the result of “strong” rare-region effects. It is noteworthy

that next-to-leading corrections provide logarithmic corrections to the power-laws. Numerical evidence of this GP regime is shown in Fig. (1b) of Ref. [12]).

(ii) Right at the percolation threshold, $q = q_{perc}$, $p \rightarrow 1$ and the distribution of finite clusters, Eq. (8), becomes a power-law. When plugged into Eq. (7) the contribution of finite clusters leads to a **logarithmic decay** with exponent $1/2$, $\rho(t) \sim [\ln(t/t_0)]^{-1/2}$, expected to hold for any $\lambda > \lambda_c(q_{perc})$, for which rare regions are active. Observe that a finite fraction of sites belongs to the (infinite) percolation cluster, where activity can survive indefinitely, therefore, the actual behavior is $\rho(t) \sim c(\lambda) + [\ln(t/t_0)]^{-1/2}$, where $c(\lambda)$ is a constant, meaning a discontinuous phase transition here. Strong evidence of such a logarithmic decay behavior is given by the inset of Fig. (1a) of Ref. [12].

(iii) For $q < q_{perc}$ there is a giant component of type-I nodes which, above the critical point given by Eq.(6), is able to sustain activity in the steady state. At criticality, a standard mean-field like contact-process behavior ($\rho(t) \sim t^{-1}$) is expected and has been numerically verified (Fig. (1a) in [12]). On the other hand, in the active region, the existence of a percolating cluster implies a stationary density $\rho(q, \lambda)$. Besides this giant component some other finite type-I clusters do exist: the relaxation in such clusters gives rise to anomalously slow relaxation toward $\rho(q, \lambda)$, analogous to that of regime (i) [17].

(iv) Below the GP (region (i)), at some value of λ , and for any value $q > q_{perc} = 2/3$, starts a different region. Here, the finite clusters, which were locally supercritical in phase (i) become typically sub-critical. Nevertheless, the connectedness of finite clusters (as well as the local control parameter) varies from cluster to cluster and, although most of them are locally sub-critical, there still may form rare clusters with an over-average mean degree, which (themselves or parts of them) are locally supercritical at a given λ . The extension and the characteristic extinction time of these rare regions is unbounded (although large extinction times are very improbable) and this circumstance is sufficient to induce a slower-than-exponential decay of the global density. The distribution of extinction times which are related to the geometry of rare regions is extremely difficult to estimate analytically. Nevertheless it is expected to decay much more rapidly than the power law characteristic of phase (i) and, correspondingly, the density is expected to decay faster than any power of t (but slower than exponentially). In this case we speak of *weak rare-region effects*.

Numerical results, as shown in Fig. 2 and Fig. 3 indicate a stretched-exponential decay, $\rho(t) \sim e^{-const \cdot t^a}$ with exponents a varying from values close to 1, for small λ , to very small values (converging to 0) for λ approaching the GP. Note, that in the limit of vanishing exponent the stretched exponential becomes a power-law.

We can use Eq. (7) the other way around and estimate the kernel as a function of the resulting convolu-

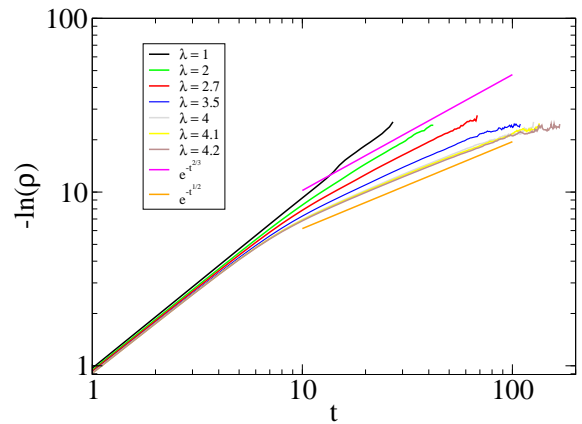


FIG. 2. (Color online) Stretched exponential decay of ρ vs t in region (iv) for $N = 10^6$, $q = 0.9$, $r = 0$ and various values of λ (which increase from top to bottom curves in the figure). As a reference, straight lines correspond to $\rho(t) \sim \exp(-ct^{2/3})$ (top) and $\rho(t) \sim \exp(-ct^{1/2})$ (bottom).

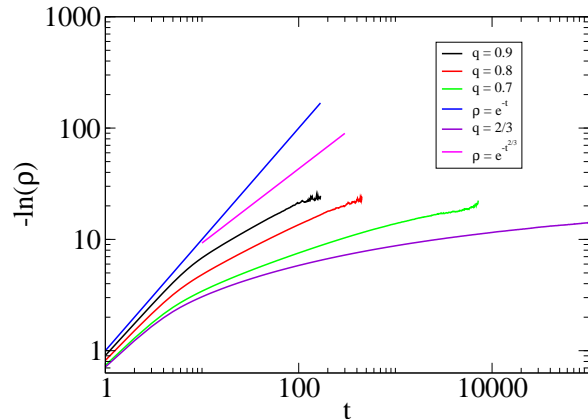


FIG. 3. (Color online) Stretched exponential decay of ρ vs t in region (iv) for $N = 10^6$, $\lambda = 4.2$ and various values of q (which decrease from top to bottom curves in the figure). As a reference, straight lines correspond to $\rho(t) \sim \exp(-t^{2/3})$ (bottom) and $\rho(t) \sim \exp(-t)$ (top), respectively. The closer q to the percolation threshold, the larger the probability to have long surviving clusters, and hence the slower the decay.

tion. Indeed, writing the integral in Eq. (7) in terms of extinction times rather than the size s of rare regions and applying the saddle point approximation we obtain that an overall stretched exponential decay for $\rho(t)$ (as measured numerically) implies the asymptotic form $P(\tau) \sim \exp(-const \cdot \tau^{a/(1-a)})$ for the distribution of extinction times.

For values of $q < 2/3$, above the percolation threshold, the density decay towards the absorbing state is still expected to be dominated by the rare finite clusters which are present beside the spanning cluster and to be of stretched-exponential type, as indeed observed numerically (results not shown).

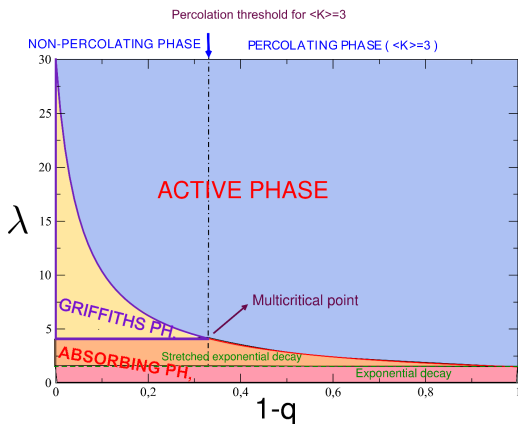


FIG. 4. (Color online) Phase diagram for $r > 0$. In contrast to the $r = 0$ case, the active phase extends all the way to $q = 1$. Otherwise, the phase diagram is very similar to the one for $r = 0$, including a Griffiths phase and a region of weak rare region effects.

(v) For $\lambda < \lambda(q = 0)$ and any q , no cluster can be super-critical, but still different effective values of τ compete, giving rise, again, to stretched exponential behavior. For very small values of λ , i.e. deep into the absorbing phase the decay for all clusters is so fast, that the distribution of τ becomes very narrow and the decay is very close to purely exponential (and therefore the exponent of the stretched exponential becomes very close to unity).

2. Case $r > 0$

When nodes of type-II conserve some reduced spreading capability ($r > 0$) the features of the phase-diagram remain essentially unchanged (see Fig. 4), except for an important qualitative modification: even in the phase where type-I nodes do not percolate a global percolation is guaranteed by type-II nodes. One consequence is that an active phase exists even when $q > q_{perc}$ for values of λ larger than $\lambda_c(q)$ approximately given by Eq. (6). The Griffiths phase is limited by such a line above and $\lambda_c(q_{perc})$ below. For smaller values of the spreading rate λ one still expects a stretched exponential decay and, below $\lambda_c(q = 0)$ a pure exponential behavior. In Fig. 5 results of numerical simulations for $r = 0.05$ and $q = 0.9$ confirm these expectations. Observe the existence of some curvature for the decaying curves in the double logarithmic plot; this is due to the existence of logarithmic corrections to scaling.

Summing up, optimal fluctuation arguments explain all numerical findings for both $r = 0$ and $r > 0$. *Rare*

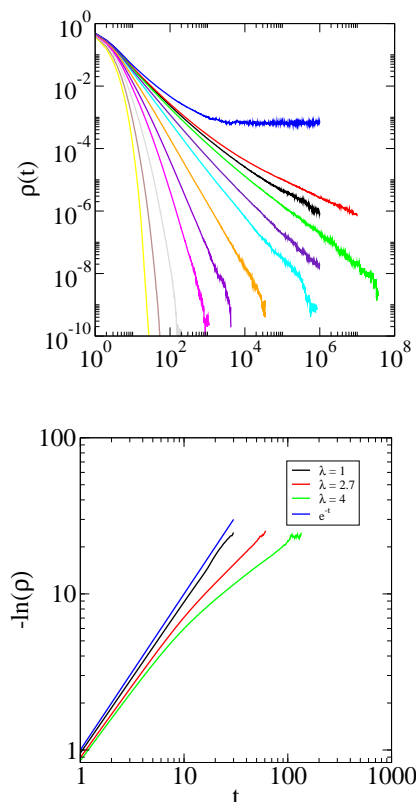


FIG. 5. (Color online) Decay of $\rho(t)$ for $q = 0.9$ and $r = 0.05$ ($N = 10^7$). The top plot highlights the presence of a generic power-law decay. Values of λ are (from top to bottom curves) 11, 10.34, 10.2, 10.95, 9.8, 7.6, 4.5, 2.7, 1. The bottom plot reveals the presence of a stretched exponential regime for $\lambda \lesssim 4.5$. Values of λ increase from top to bottom curves. The straight line corresponds to the exponential decay $\rho(t) = \exp(-t)$.

regions play an important role in almost all phase space, giving rise to generic slow decay of activity.

The nature of the transition between the active phase and the Griffiths phase is expected to be of activated scaling type, i.e. logarithmic decay is expected (see Sect. III B 1). Indeed, our simulation results suggest activated critical behavior but computing accurately the corresponding exponents remains an open challenge. Let us remark that recently, a strong disorder renormalization group calculation has been performed for Erdős-Rényi networks, with the conclusion that a strong-disorder fixed point emerges even in this infinite dimensional topology [21]. Comparing numerical results with the theoretical predictions in [21] is left for future work.

D. QCP behavior on scale-free networks

It is possible to predict what happens when the QCP dynamics takes place on some other, more complex, topology. We hypothesize that strong rare-region effects (i.e. GP) occur in the fragmented phase of networks with a finite percolation threshold: if over-active sites cannot

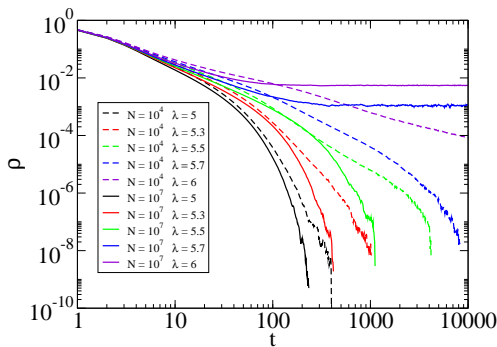


FIG. 6. (Color online) Time decay of the average activity ρ for the QCP on a scale-free network built using the Uncorrelated Configuration Model [23]. The degree distribution decays as $P(k) \sim k^{-2.5}$. Solid lines are for $N = 10^7$, dashed lines are for $N = 10^4$. Values of λ decrease from top to bottom curves. Notice that, while for $N = 10^4$ a slow decay occurs at the transition, as the system size is increased ($N = 10^7$) the typical behavior of the pure systems is observed.

form rare isolated regions, then rare-region effects do not appear. Example of such networks are the ransom ER above or structured scale-free networks [22]. On the other hand, if the percolation threshold decreases with system size and vanishes in the thermodynamic limit (as is the case in standard scale-free networks [1]) only weak rare-region effects are expected.

Numerical evidence of this last assertion is provided in Fig. 6. It corresponds to a simulation of the QCP on scale-free networks (generated using the uncorrelated configuration model [23]). Apparently, power-law generic decay is observed when the network is small ($N = 10^4$); however, as the size is increased ($N = 10^7$) the transition becomes similar to the usual transition for the pure contact process, with no track of generic power-law decay, i.e. no evidence of a Griffiths phase.

III. EFFECTS OF TOPOLOGICAL DISORDER

A. General considerations

In what follows, we assume that the infection rate λ_i for site i is identical for all sites and explore the possibility of rare region effects induced solely by the topological irregularities. It is important to remark that, still, the infection rate through any given *link* is non-homogeneous if the degrees of sites are heterogeneous.

The “local” critical control parameter in any given region depends on the connectedness of sites in that region (see Eq. (2)), and therefore heterogeneous networks are susceptible to exhibit rare region effects: clusters with an over-average local connectedness would have a lower local critical control parameter and hence they could be

locally active even if the system is globally in the absorbing phase.

The effects of *topological disorder* are less clear than those of intrinsic node disorder. See, for instance, the contradiction between numerical results and the Harris-Luck criterion for CP on two-dimensional Voronoi-Delaunay network (the latter predicting topological disorder to be relevant and the former showing the contrary [24]).

To shed some light on these problems, let us first consider the CP on a network with bimodal degree distribution, $P(k) = p\delta(k - k_1) + (1 - p)\delta(k - k_2)$ with $k_1 \gg k_2$, where a priori one could expect rare active regions (with an over-density of k_1 -nodes) to exist. However, numerically we find just conventional, non-disordered, behavior with no evidence of anomalous effects for such networks. What is the reason for this apparent contradiction?

In d -dimensional lattices, disorder is known to be irrelevant for sufficiently high d , where each node has a large number of neighbors and the law of large numbers precludes rare regions from existing: each site effectively “sees” a well defined mean field, homogenous across the system. The *topological dimension* is an extension of the concept of Euclidean dimension to arbitrary graphs. It measures how the total number of nodes in a local neighborhood grows as a function of the topological distance from an arbitrary root: $N(l) \sim l^D$ [15]. For small-world networks (like the ER graph), where $N(l)$ grows (at least) exponentially with l and, consequently, the topological dimension is formally infinite. On the other hand, for disconnected graphs with no macroscopic (giant) component, like the ER graph below the percolation threshold, $D = 0$.

For networks with $D = \infty$ (as ER graphs above the percolation threshold or the bimodal graphs above), the number of nodes in a local neighborhood is large. Therefore we conjecture, in analogy with the case of lattices, that GPs cannot exist. In such networks, the “locality” (i.e. the very existence of local neighborhoods), which is a basic component of the phenomenology of rare regions is broken. This means that the exponentially growing neighborhood reduces the possibility of forming well-separated rare regions. In other words, the surface of these regions is proportional to their volume if $D = \infty$ and the number of external links through this large surface has to be below-average such that the region is isolated from the rest. As opposed to this, GPs may exist for ER below the percolation threshold. where $D = 0$ and the finite components of the network are isolated from each other.

In order to get more insight into the effects of topological disorder we have studied the CP on several types of networks with finite D by numerical simulation. We have studied Generalized *Small-World* (GSW) networks [25–33], which consist of a one-dimensional lattice and an additional set of long-range edges of arbitrary, unbounded, length. The probability that a pair of sites separated by a distance l is connected by an edge decays

with l as

$$P(l) \simeq \mathcal{N}\beta l^{-s} \quad (9)$$

for large l , where \mathcal{N} is a normalization factor enforcing the mean degree to be finite.

These networks interpolate between the case $s = 0$, which is similar to ER graphs in the sense that long edges exist with a uniform (l -independent) probability (note, however, that the underlying one-dimensional lattice ensures that the networks is always connected) and the quasi-one-dimensional network with certain fraction of next-to-nearest neighbor edges corresponding to $s = \infty$. In general, $P(l)$ decreasing with the edge length, l , results in an overall tendency toward forming clusters of consecutive sites possessing an over-average number of internal links, as occurs in the extremal case $s = \infty$. In the latter model simple considerations predict the existence of a GP. Clearly, for $s > 2$, links have a strong tendency to be local; actually the probability that a site belongs to a sub-graph that contains many internal links¹ and has no external long edge is finite in the limit $N \rightarrow \infty$. This probability is exponentially small in the sub-graph size, suggesting the possibility of strong rare region effects. On the other hand, for $0 \leq s \leq 2$, the number of sub-graphs specified above is only sub-linear in the system size, and hence they are more likely to become irrelevant in the limit $N \rightarrow \infty$.

In the following two subsections we study two different families of networks –non-regular and regular respectively– within this class of generalized small-world networks.

B. Non-regular generalized small-world networks

We have studied non-regular GSW networks which were proposed in the context of long-range percolation [25]. Consider N nodes, labeled $1, 2, \dots, N$ and let us define a distance between nodes i and j , $l = \min(|i - j|, N - |i - j|)$. All pairs of sites at distance $l = 1$ are connected with probability 1, while pairs with $l > 1$ are connected with a probability

$$P(l) = \mathcal{N}[1 - \exp(-\beta l^{-s})] \quad (10)$$

obeying Eq. (9) for large values of l .

The topological dimension of these graphs has been shown to depend on s . If $s > 2$, the average length of edges is finite, consequently, $D = 1$, whereas for $s < 2$, the average length diverges, implying that the topological dimension is formally $D = \infty$ [27, 30, 34]. In the ‘‘marginal’’ case $s = 2$, D is finite and depends on the pre-factor β (actually D grows with β ; see below) [27, 30, 35].

¹ for example a sub-graph consisting of consecutive sites and all next-to-nearest neighbor links

1. The case $s > 2$

For $s > 2$, long-edges are irrelevant, $D = 1$, and their net effect is to induce an over-density of links for some nodes, i.e. to induce a form of local quenched disorder.

For the one-dimensional QCP a strong disorder renormalization group analysis shows that the critical behavior is governed by an infinite-randomness fixed point (IRFP) where the dynamics is logarithmically slow [36, 37]. This results have been extended to higher dimensions [21, 38]. In particular, for spreading dynamics (i.e. starting from a single active site [39]) the survival probability $P(t)$ and the number $N(t)$ of active sites which are averaged over the initial site behave as

$$P(t) \sim \ln(t/t_0)^{-\tilde{\delta}}, \quad N(t) \sim \ln(t/t_0)^{\tilde{\eta}}. \quad (11)$$

Instead, initializing the system from fully active state, the density of active sites decays as

$$\rho(t) \sim \ln(t/t_0)^{-\tilde{\alpha}}. \quad (12)$$

At the IRFP in one dimension the critical exponents are exactly known $\tilde{\delta} = \tilde{\alpha} = (3 - \sqrt{5})/2$, $\tilde{\eta} = \sqrt{5} - 1$ [36].

On the grounds of universality we expect the same critical dynamics as for the one-dimensional QCP with node-dependent transition rates [8, 36]. In order to check this conjecture we have investigated the model with $s = 3$ and $\beta = 2$ with extremely long simulations (2^{28} Monte-Carlo steps) on lattices of size $N = 10^5$. We measure the density decay starting from a fully active state and determine the effective decay exponent (by assuming it is a power-law and using local slopes in a log-log plot) as

$$\alpha_{\text{eff}}(t) = -\frac{\ln[\rho(t)/\rho(t')]}{\ln(t/t')}, \quad (13)$$

where $\rho(t)$ and $\rho(t')$ are neighboring data points. Other effective exponents are measured analogously. Numerical simulations in the sub-critical region confirm the presence of a Griffiths phase with algebraic dependence on time in the range: $\lambda = 2.70 - 2.78$ (Fig.7).

Results at the transition point are found to be compatible with Eq. (12) with the 1d QCP exponent $\tilde{\alpha} = (3 - \sqrt{5})/2 \approx 0.382$ in the critical point at $\lambda_c = 2.783(1)$. Indeed, in Fig. 9 the effective exponents (local slopes) $\bar{\alpha}_{\text{eff}}(t)$ against time. As a comparison we also plot the effective exponents $\bar{\delta}_{\text{eff}}(t)$ obtained for the one-dimensional QCP on lattices of size $L = 10^5$ with bimodal disorder distribution (4) ($r = 0.3$, $q = 0.2$; observe that this comparison makes sense since for the QCP the exact relation $\alpha = \delta$ holds, i.e. the rapidity reversal symmetry is not broken [13]). The critical point of the 1d QCP is found to be located at $\lambda_c = 5.24(1)$, in agreement with [40]. As can be seen, the convergence towards a value compatible with the expected asymptotic value is very slow (see red dot on the ordinate in the inset of Fig. 9, corresponding to the $t \rightarrow \infty$ limit) owing to the considerable time scale t_0 in Eqs. (11-12). As a consequence, in case of an activated scaling, if neither λ_c nor the critical exponents are

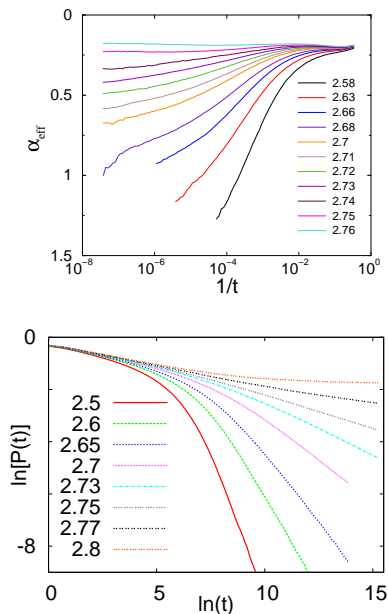


FIG. 7. (Color online) Top: Local slopes of the density decay in networks with $s = 3$ and $\beta = 2$ for different values of λ in the Griffiths phase Bottom: Time-dependence of the survival probability in the same networks. Numbers shown correspond to lines from bottom to top.

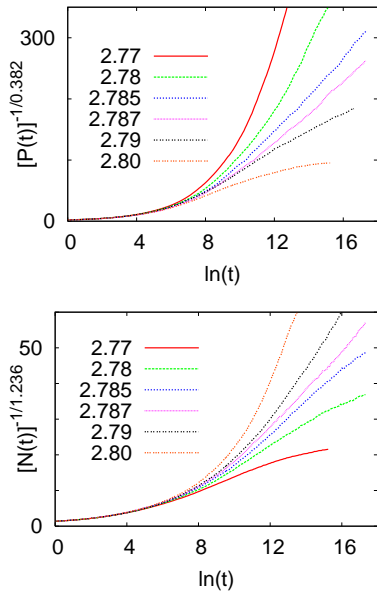


FIG. 8. (Color online) Top: Time-dependence of the survival probability in seed simulations in the network with $s = 3$ and $\beta = 2$ (numbers shown correspond to lines top bottom). Bottom: The corresponding number of active sites in (numbers shown correspond to lines from bottom to top). A straight line in these plots correspond to the critical point as with activated scaling with $\tilde{\delta} \approx 0.382$ and $\tilde{\eta} \approx 1.236$.

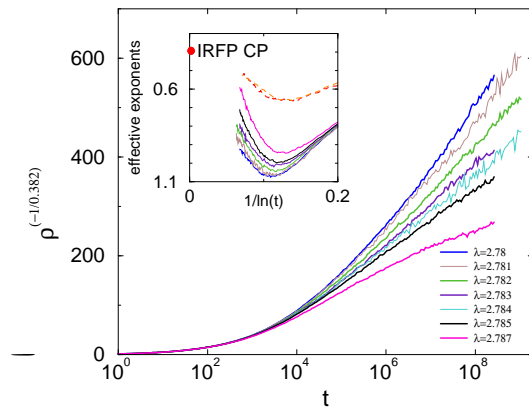


FIG. 9. (Color online) Density decay results in the network with $s = 3$ and $\beta = 2$ illustrating the existence of activated (logarithmic) scaling at criticality (numbers shown correspond to lines from top to bottom). Inset: local slopes of the same data (lower curves), and local slopes of the survival probability in the critical 1d QCP simulations. Slow convergence towards a value compatible with the IRFP value of the 1d QCP can be observed.

known a priori the usual method of inspecting the local slopes in order to estimate exponents is mostly useless and one has to resort to more complex methods [38].

Finally, results for $N(t)$ and $P(t)$ shown in Fig. 8 are also compatible with Eqs. (11) with the IRFP exponent values.

2. The marginal case $s = 2$

For $s = 2$ the topological dimension increases continuously with β . In Ref. [35], $D(\beta)$ has been estimated for different values of β . For the values of β studied in this paper 0.1, 0.2, 1 the dimensions are 1.104(3), 1.212(5), 2.35(2), respectively. We have studied the CP in these cases, expecting an absorbing phase transition at some β -dependent critical point $\lambda_c(\beta)$. It is reasonable to assume that the addition of edges to a network lowers λ_c , i.e. $\lambda_c(\beta)$ is monotonically decreasing with β . Consequently, the model with some fixed β ($0 < \beta < \infty$) must be in the active phase, if $\lambda > \lambda_c(0) = 3.297848(22)$ (the critical point of the one-dimensional CP, see [13]) and must be inactive, if $\lambda < 1$ (the critical point of the complete graph described by the mean-field equations, see Eq. (2)). Therefore one can predict: $1 \leq \lambda_c(\beta) \leq \lambda_c(0)$, with a possible GP also in this range. Note that the range $[1, \lambda_c(\beta)]$ where a GP can emerge on the inactive side of the critical point shrinks upon enlarging β , making it difficult to numerically observe GPs for large values of β . On the other hand, the smaller the value of β (and hence the smaller the mean degree of nodes) the weaker its influence of the pure system fixed point and the larger times are needed in the simulations in order to see the true asymptotic behavior.

We have studied the dynamics of CP on these networks via density decay as well as spreading simulations from a single active seed for different β values around the corresponding phase transition points (system-sizes $L = 10^5 - 10^6$ and up to $t_{\max} \leq 10^8$ Monte Carlo steps).

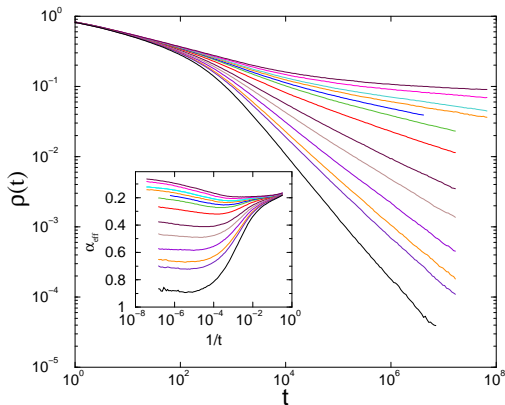


FIG. 10. (Color online) Density decay in the $\beta = 0.1$ network of linear size $L = 10^6$ for $\lambda = 1.287, 1.29, 1.291, 1.293, 1.295, 1.297, 1.3, 1.302, 1.303, 1.304, 1.3048, 1.306, 1.307$ (from bottom to top), illustrating the existence of a Griffiths phase. The inset shows the corresponding continuously-varying local slopes.

As can be seen in Fig. 10 for $\beta = 0.1$, the density decays algebraically with λ -dependent exponents in an extended range of λ (results of seed simulations for $\beta = 0.2$ also support the existence of a GP in agreement with the results for density decay (see Fig. 3 of [12])).

The calculated effective exponents $\alpha_{\text{eff}}(t)$ for $\beta = 0.1$ do not level-off for large times (see insets of Fig. 10) instead a slow drift proportional to $1/\ln(t)$ can be observed. The functional dependence of the effective exponent can be well fitted by

$$\alpha_{\text{eff}}(t) = \alpha - a/\ln(t) \quad (14)$$

suggesting the presence of logarithmic corrections of the form: $\rho(t) = t^{-\alpha} \ln^a(t)$. The possibility of such logarithmic corrections to power laws in the GP was already pointed out in case of the QCP [7] and arises naturally using optimal fluctuation arguments (see above). The relation $\alpha = \delta$ seems to hold in accordance with the rapidity reversal symmetry of the CP [41]. The phenomenological theory of the GP (see [7]) predicts that the number of active sites in surviving samples, i.e. $N(t)/P(t)$ grows as a power of $\ln t$, implying $\eta = -\delta$ [7]. By extrapolating the effective exponents to $t \rightarrow \infty$ we have found that this relation is satisfactorily fulfilled.

As discussed above a Griffiths phase is usually accompanied by a logarithmically slow $-$ activated dynamics $-$ at criticality (see in Eqs. (11-12)). We expect this scenario to hold for $\beta > 0$, with possibly modified critical exponents compared to the case $s > 2$. Results of numerical

simulations for $\beta = 0.2$ are in accordance with these expectations but without knowing the critical exponents it is hard to accurately estimate the critical point location. We applied a method of Ref. [38], based on the assumption that the leading correction to scaling comes from the time scale t_0 in Eqs. (11-12), which is the same for different quantities. At criticality both $\ln[P(t)]$ and $\ln[N(t)]$ are thus asymptotically proportional to $\ln[\ln(t/t_0)]$. Plotting $\ln[N(t)]$ against $\ln[P(t)]$ the data at the critical point must fit to a straight line with a slope $-\bar{\eta}/\bar{\delta}$ (see Fig. 11). On the other hand in the GP (actually in all the absorbing phase) the slope tends to $+1$ whereas in the active phase it tends to $-\infty$. This allows us to obtain a rough estimate of the critical point: $\lambda_c = 2.85(1)$.

Unfortunately, the ratio $\bar{\eta}/\bar{\delta}$ varies rather sensitively with λ around the suggested critical point. The data at $\lambda = 2.84, 2.85, 2.86$ give the ratio estimates 1.5(1), 1.9(1), 2.6(1), respectively, making it very difficult to obtain reliable estimates (for comparison, remind that the corresponding ratio of the 1d QCP is $\bar{\eta}/\bar{\delta} \approx 3.236$).

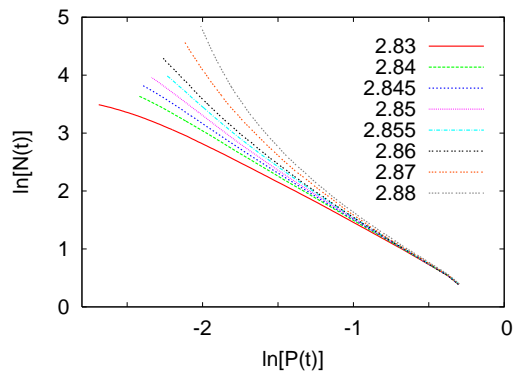


FIG. 11. (Color online) The logarithm of the number of particles plotted against the logarithm of survival probability for different values of λ in networks of size $N = 10^6$ for $s = 2$ and $\beta = 0.2$ (numbers shown correspond to lines from bottom to top) A straight line in this plot signals the transition point.

Having an estimate of λ_c at our disposal, we turned to the estimation of $\bar{\alpha}$, $\bar{\delta}$ and $\bar{\eta}$ separately. Assuming that the survival probability has the asymptotic time dependence $P(t) \simeq \text{const} \times [\ln(t/t_0)]^{-\bar{\delta}}$, we obtain that the effective exponent $\bar{\delta}_{\text{eff}}(t) \equiv -\frac{d \ln P(t)}{d \ln(\ln t)}$ has the following dependence on time:

$$\bar{\delta}_{\text{eff}}(t) = \bar{\delta} \left(1 + \frac{\ln t_0}{\ln(t/t_0)} \right). \quad (15)$$

As can be seen, the deviation from the true value is considerable whenever $\ln t$ is not much greater than $\ln t_0$. A similar form can be obtained for $\bar{\alpha}$ and $\bar{\eta}$ as well. We have calculated the effective exponents from numerical data and fitted the form in Eq. (15) to them in the domain $1/\ln(t) < 0.12$ where the other corrections are expected to be negligible. These numerical data and the fitted curves can be seen in Fig. 12. The extrapolated

critical exponents, which can be read off from the intersection with the y -axis express considerable error, due to the uncertainty of the location of the critical point even though the large simulation efforts applied.

The exponent $\bar{\delta}$ is found to increase with β , leaving the value $\bar{\delta}(\beta = 0) \approx 0.382$ of QCP, whereas $\bar{\eta}$ is less accurate, decreasing from the value $\bar{\eta}(\beta = 0) \approx 1.236$ of the QCP.

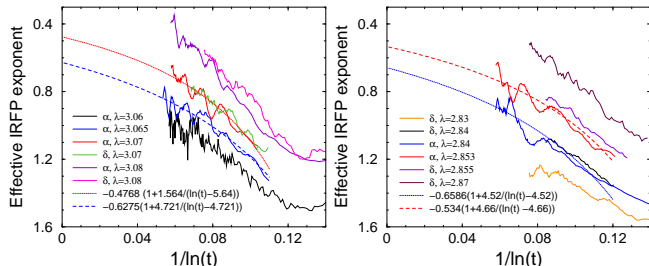


FIG. 12. (Color online) Numerically calculated effective exponents $\bar{\delta}_{\text{eff}}(t)$ and $\bar{\alpha}_{\text{eff}}(t)$ (solid lines) plotted against $1/\ln t$ and the curves given in Eq. (15) fitted to them (dotted lines) in the vicinity of the critical point for $\beta = 0.1$ (left) and $\beta = 0.2$ (right) (parameters shown correspond to lines from bottom to top).

We have also studied the evolution of the growing cluster in seed simulations by measuring its diameter: $R(t) = \sqrt{\langle \sum_i n_i(t) l_i^2(t) / \sum_i n_i(t) \rangle}$, where the occupation number $n_i(t)$ is 1(0) if site i at time t is active(inactive), l_i is the length of shortest path between site i and the initial site and $\langle \cdot \rangle$ denotes disorder average over samples where the process is surviving up to time t . According to the phenomenological theory of the GP, the spread $R(t)$ grows as a power of $\ln t$. Actually, the critical point of the 1d QCP strong disorder renormalization group predicts that $R(t) \sim (\ln t)^{1/\psi}$ with the exponent $\psi = 1/2$ [36]. Indeed, we have found the behavior

$$R(t) \sim (\ln t)^{1/\psi}. \quad (16)$$

at criticality with ψ not far from $1/2$ for $\beta = 0.2$.

The picture above changes as β is further increased. Indeed, our numerical observations show that, as argued above, the size of the GP shrinks upon enlarging β . Actually, for $\beta \geq 1$ we can no longer observe a GP and we obtain conventional power-law dynamics at the suggested critical point rather than activated dynamics. At a numerical level, however, we cannot rule out the possibility of the presence of a GP of vanishing width which persists to exist for any finite β and is accompanied by activated critical dynamics which can be observed only at time scales that are well beyond the realm of numerically attainable ones.

With increasing β , the mean degree increases and it is tempting to compare the numerical results with those for a related model which can be regarded as the “annealed” counterpart of networks with quenched topological irregularities. In that model, referred to as CP with Lévy-flights [42, 43], activation is possible not only at adjacent

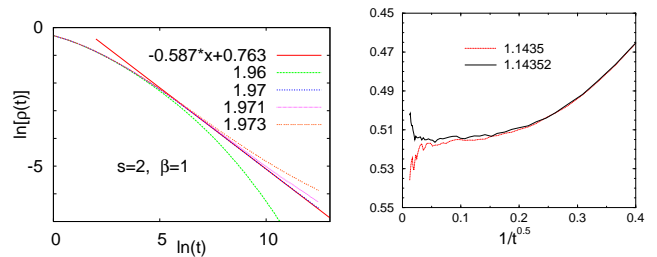


FIG. 13. (Color online) Left: Density time-decay in MC simulations started from the fully active state in networks with $s = 2$ and $\beta = 1$. Right: Effective exponents $\alpha_{\text{eff}}(t)$ for $s = 2$, $\beta = 5$ in the vicinity of the transition point (parameters shown correspond to lines from bottom to top).

sites but at any site, chosen at any time step (“annealed links”) with a probability decaying with the distance as

$$P(r) \sim r^{-d-\sigma}. \quad (17)$$

Field theoretical analyzes proved that for dimensions above $d_c = 2\sigma$, the critical exponents vary continuously with σ , while below such a critical dimension they coincide with mean-field critical exponents (up to logarithmic corrections at $d = d_c$) [44]. In one dimension, this means that non-trivial, σ -dependent exponents are expected if $\sigma > 1/2$, whereas they are stuck to the mean-field values if $\sigma < 1/2$. So, it is reasonable to compare the quenched model to the annealed one with the same decay exponent, i.e. $s = \sigma + 1$. For $\sigma = 1$ corresponding to $s = 2$, the numerical estimate of the density-decay exponent is $\alpha = 0.52(3)$ [45]. This is quite close to the estimated critical exponents of the corresponding quenched model with large β , see Fig. 13. At $\beta = 5$, for which we have the most accurate estimates, $\alpha = 0.515(20)$.

As can be seen from the numerical results, the behavior of the quenched model is similar to that of the annealed one for large enough β . This similarity is, however, deteriorates for small β , which is easy to understand on an intuitive level, since for $\beta < 1$, there is a diverging number of backbone links ($O[N^{1-\beta}]$) [25, 27], over which no long-range activation can occur, hence the approximation by an effective CP with Lévy-flight must be inappropriate.

3. The case $s < 2$

In the case $s < 2$ we choose the normalization factor \mathcal{N} in Eq. (9) such that the mean degree is $\langle k \rangle = 3$ for all values of s . Simulations show that the trend observed for $s = 2$ and large values of β is continued. Namely, no signs of a GP can be found and the critical dynamics are of conventional power-law type. Taking into account the strong finite-size corrections as well as the possibility of logarithmic corrections at $s = 3/2$ (which corresponds to $d = d_c$ in the annealed model) the results (not shown) for $s \leq 3/2$ are compatible with the mean-field value $\alpha = 1$

of the decay exponent in the contact process with Lévy-flights. As expected, the estimated critical exponents do not seem to depend on the mean degree $\langle k \rangle$ but on the index s . For example at $s = 1.75$, the estimated value is $\alpha = 0.75(1)$ (not shown) in agreement with the expected value of the decay exponent of the annealed model at this point is $\alpha \approx 0.72(5)$ [45].

C. 3-regular random networks

In the networks studied so far the degree of nodes is heterogeneous. In the following we consider networks with a topological disorder which is even weaker in the sense that the degree of all nodes is the same (3 in our case).

In order to keep the topological dimension finite we need the probability of long edges to decay according to Eq. (9) with $s = 2$. Such 3-regular random networks can be constructed in the following way [33]. Initially, let us have a one-dimensional periodic lattice with N vertices, all of them are of degree 2. Vertices of degree 2 will be briefly called “free vertices”. Let us assume that N is even and k is a fixed positive integer. Now, a pair of free vertices between which the number of free vertices is $k-1$ (the number of non-free vertices can take any value) is selected randomly with uniform probability from the set of all such pairs and this pair is then connected by a link. That means, for $k = 1$, neighboring free vertices are connected, for $k = 2$ next-to-neighboring ones, etc. This step, which raises the degree of two free vertices to 3 is then iterated until all vertices become of degree 3. (The last $2(k-1)$ free vertices are paired in an arbitrary way.) Remarkably, as shown in Appendix B, the probability of long-distance edges is given by Eq. (9) with $s = 2$ for all k and the pre-factor is $\beta = k/2$. The topological dimension for $k = 1$ has been shown to be $D(k = 1) = 2$ while for $k = 2$ the numerical estimate is $D(k = 2) = 2.27(2)$ [33].

1. Results

As expected, simulation results obtained for $k = 1, 2$ are in line with those obtained for non-regular random networks with $s = 2$ and different values of β . For $k = 1$ (corresponding to $\beta = 0.5$ above) we can observe a GP, where the density decays algebraically (up to possible logarithmic corrections) with exponents continuously varying with λ , see Fig. 14, and activated scaling (not shown) at criticality.

On the other hand, for $k = 2$ (corresponding to $\beta = 1$ above), finite size effects are stronger because the diameters of the networks are smaller. The density decay results are shown in Fig. 15. As can be seen from the local slopes, the existence of GP is questionable, instead a conventional critical phase transition appears at $\lambda_c = 2.1583(1)$ with the decay exponent $\alpha \simeq 0.52(5)$,

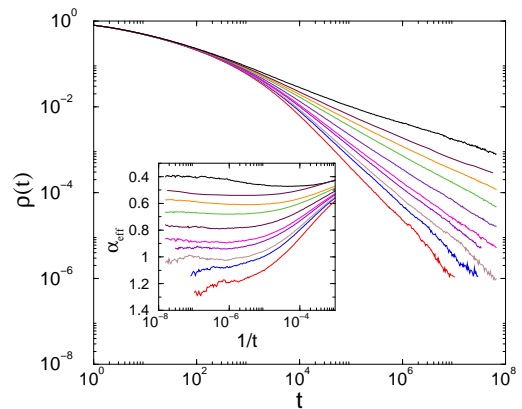


FIG. 14. (Color online) Density decay in the $k = 1$ network of size $L = 10^6$ from $\lambda = 2.53, 2.535, 2.537, 2.541, 2.543, 2.548, 2.554, 2.558, 2.562, 2.57$ (from bottom to top). The inset shows the corresponding local slopes.

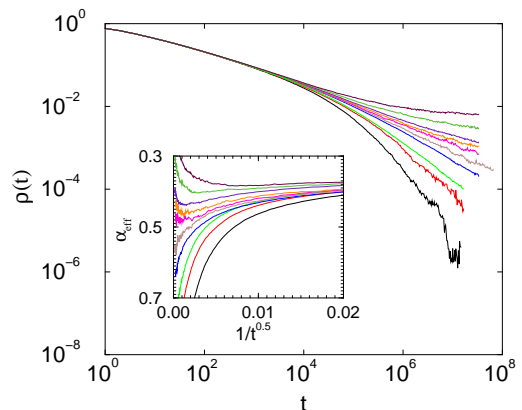


FIG. 15. (Color online) Density decay in the $k = 2$ network for $L = 10^7$ for $\lambda =$ from $\lambda = 2.156, 2.157, 2.1575, 2.1581, 2.1583, 2.1584, 2.1586, 2.1588, 2.1593, 2.1598$ (from bottom to top). The inset shows the corresponding local slopes.

which is again close to the corresponding value of the annealed model.

IV. DISCUSSION

In summary, aimed at studying the effect of disorder on propagation phenomena occurring on networks, we have investigated the simple contact process on top of different network architectures. First, we have considered a quenched contact process, in which the infection rate is node-dependent, and we have analyzed it on Erdős-Rényi random graphs. As a simple example we have taken a bimodal disorder distribution in which nodes infect their neighbors either with high or low (even vanishing) probability. Localized rare regions, with an over-average infection rate can emerge in the network when their probability is below the network percolation threshold. In such

a case strong rare region effects appear. These include a Griffiths phase and a rich phase diagram characterized by generically slow decay of activity. The main reason behind such anomalous behavior is that rare-regions are exponentially rare, but being locally active, they survive for exponentially large times. The convolution of these two effects lead generically to slow decay. Simple “optimal fluctuation arguments” have allowed us to understand the rich emerging phase diagram and to characterize analytically the emerging regimes. In particular, we distinguish between “strong” rare-region effects appearing when the process is locally super-critical, and “weak” rare-region effects, occurring when the process is predominantly locally sub-critical.

Similar effects may appear on other topologies as long as the percolation threshold is finite. For instance, for standard scale free networks in which the percolation threshold is known to vanish in the large system-size limit, no GP can exist.

In the second part of the paper we keep the infection rate constant at all nodes, and focus the attention on the effect of network topological heterogeneity. We conjecture that, at least for the dynamical processes we have studied, Griffiths phases and other rare-region effects can appear if the network topological dimension is finite. Otherwise, (i.e. for infinite dimensional architectures) the very concept of “local neighborhood” does not make sense; the frontier of any cluster covers almost completely the whole network. We have carefully analyzed different generalized small-world networks with finite topological dimension: they consist of a one-dimensional lattice, with additional long-distance links, which exist with a probability that decays with their length l as βl^{-s} . For effectively short ranged links (i.e. $s > 2$) long-distance edges are mostly irrelevant: the topological dimension remains $D = 1$. Their main effect is to create quenched disorder. It is therefore not surprising that the results of our computer simulations show results compatible with the one-dimensional contact process with quenched disorder.

For $s < 2$, however, no Griffiths phase emerges, and the critical behavior is of the conventional type with exponents close to those of the one-dimensional CP with Lévy-flights. In the marginal case, $s = 2$ and for small value of β we observe a GP and an activated critical behavior with β -dependent exponents. By increasing β the width of GP shrinks and for large enough β it seems to disappear and the critical behavior is found to be conventional.

It would be interesting to study if slow-relaxation and other rare-region effects appear for dynamical processes other than the CP, such as the voter model [19] or in GSW-s built on higher dimensional regular lattices.

The general aspects of the results obtained in this work might be relevant for recent developments in dynamical processes on complex networks such as the simple model of “working memory” [46], social networks with heterogeneous communities [47] or slow relaxation in glassy systems [48].

ACKNOWLEDGMENTS

This work was supported by the HPC-EUROPA2 pr. 228398, HUNGRID, Hungarian OTKA (T77629,K75324), OSIRIS FP7, Junta de Andalucía proyecto de Excelencia P09-FQM4682, MICINN-FEDER project FIS2009-08451 and by the János Bolyai Research Scholarship of the Hungarian Academy of Sciences (R.J).

Appendix A: Pair approximation for the pure Contact Process

Using the notation of [18], let us call: ρ the probability to have an occupied site $u = p(1, 1)$ the probability to find a pair of occupied sites. $z = p(0, 0)$ the probability to find a pair of empty sites $w = p(1, 0) = p(0, 1)$ the probability to have in a pair 1 occupied and 1 empty site. Normalization imposes

$$u + z + 2w = 1. \quad (\text{A1})$$

Using the Bayes rule $P(1|1) = u/\rho$; $P(0|1) = w/\rho$, $P(1|0) = w/(1 - \rho)$, and $P(0|0) = z/(1 - \rho)$ for the conditional probabilities. Equivalently,

$$\begin{aligned} w &= p(1, 0) = (1 - \rho)P(1|0) = (1 - \rho)(1 - \rho - P(0|0)) \\ &= (1 - \rho)(1 - \rho - z/(1 - \rho)) \\ &= 1 - \rho - 1 + u + 2w, \end{aligned} \quad (\text{A2})$$

from where, again, we obtain $w = \rho - u$, leaving only 2 unknowns, say ρ and u .

The death rate of any occupied site is fixed to 1, while the “infection rate” of a given site with j occupied neighbors is proportional to $\lambda j/k$. More specifically, the transition rate for a state with a central empty site and j occupied neighbors is given by:

$$\begin{aligned} &\lambda \frac{j}{k} \frac{k!}{j!(k-j)!} [P(1|0)]^j [P(0|0)]^{k-j} P(0) = \\ &\frac{j}{k} \frac{k!}{j!(k-j)!} w^j z^{k-j} (1 - \rho)^{k-1} \end{aligned} \quad (\text{A3})$$

and a similar expression for the death rate. Using this, it is straightforward to obtain

$$\begin{aligned} \dot{\rho}(t) &= \frac{\lambda}{(1 - \rho)^{k-1}} \sum_{j=1}^k \frac{j}{k} \frac{k!}{j!(k-j)!} w^j z^{k-j} - \rho \\ &= \frac{\lambda}{(1 - \rho)^{k-1}} w(w + z)^{k-1} - \rho \end{aligned} \quad (\text{A4})$$

where the combinatorial factor stands for the number of ways in which an empty site can be infected by j occupied neighbors (with $j \in [1, k]$). The factor j/k stems from the infection rate. On the other hand, the negative term represents death events (notice that the term $-\rho$ could also be obtained by adding up all the possible

contributions from all the possible configurations of its neighbors). Using that $w + z = 1 - \rho$, we obtain the final expression:

$$\dot{\rho}(t) = \lambda w - \rho = \lambda(\rho - u) - \rho. \quad (\text{A5})$$

Similarly, for u :

$$\begin{aligned} \dot{u}(t) = & \frac{\lambda}{(1-\rho)^{k-1}} \sum_{j=1}^k \frac{j^2}{k} \frac{k!}{j!(k-j)!} w^j z^{k-j} \\ & - \frac{1}{\rho^{k-1}} \sum_{j=1}^k j \frac{k!}{j!(k-j)!} u^j w^{k-j} \end{aligned} \quad (\text{A6})$$

where the extra factor j reflects the fact that every-time a site (having j occupied neighbors) becomes occupied (resp. empty), j pairs are created (resp. annihilated).

For the first term in the r.h.s. we have not found any closed expression accounting for the sum, while, for the second one, using that $u + w = \rho$, it is possible to obtain a simplified form:

$$\dot{u}(t) = \frac{\lambda}{(1-\rho)^{k-1}} \sum_{j=1}^k \frac{j^2}{k} \frac{k!}{j!(k-j)!} w^j z^{k-j} - ku. \quad (\text{A7})$$

Despite of the cumbersome aspect of Eq.(A7), it is possible to perform a linear stability analysis of the steady state solution of the set of equations Eq.(A5) and Eq.(A7) without finding explicitly their analytical solution. Actually, from Eq.(A5), the steady state obeys $\lambda(\rho - u) = \rho$, and hence, $\rho - u = \rho/\lambda$, and

$$u = \frac{\lambda - 1}{\lambda} \rho. \quad (\text{A8})$$

Evaluating Eq.(A7) at linear order in ρ , only the term $l = 1$ contributes to the series:

$$\begin{aligned} \lambda \frac{1}{k} k w z^{k-1} &= ku \\ \lambda(\rho - u)(1 - 2\rho + u)^{k-1} &= ku. \end{aligned} \quad (\text{A9})$$

Plugging here the result above

$$\rho = k \frac{\lambda - 1}{\lambda} \rho \quad (\text{A10})$$

from where

$$k(\lambda - 1) = \lambda \quad (\text{A11})$$

indicating that the critical point is located at

$$\lambda_c = \frac{k}{k-1}. \quad (\text{A12})$$

Appendix B: Pre-factors of 3-regular graphs

Here we calculate the pre-factor $\beta(k)$ appearing in the asymptotic expression of the probability $P(l)$ for 3-regular random graphs. Consider the constructing procedure described in the text and assume that the initial one-dimensional lattice is infinitely large. When a new edge is created, the number of free vertices is reduced by 2. So when the fraction of free vertices is reduced by an infinitesimal amount from c to $c - dc$, this corresponds to the generation of a fraction $dc/2$ of the long edges. The mean length of effective short edges $\langle \xi \rangle$ (i.e. distances between neighboring free vertices) is $1/c$, so it is plausible to assume that the probability distribution of ξ has the scaling property $\pi_c(\xi) = c\tilde{\pi}(\xi c)$ when $c \rightarrow 0$. The length l of a generated new link is the sum of k short edges, therefore

$$\langle l \rangle = k/c \quad (\text{B1})$$

and its probability $P_c(l)$ has the same scaling property as $\pi_c(\xi)$. We can write for the probability that in the network (after finishing the construction procedure) two sites in a large distance l are connected by a link:

$$\begin{aligned} P(l) &\simeq \int_0^{c_0} P_c(l) \frac{dc}{2} \simeq \frac{1}{2} \int_0^{c_0} c \tilde{P}(lc) dc \\ &= \frac{1}{2l^2} \int_0^{lc_0} x \tilde{P}(x) dx \simeq \frac{1}{2l^2} \langle x \rangle = \frac{k}{2} l^{-2}, \end{aligned} \quad (\text{B2})$$

where $1/l \ll c_0 \ll 1$ and we have used Eq. B1. Thus, we obtain

$$s = 2 \quad \text{and} \quad \beta = \frac{k}{2}. \quad (\text{B3})$$

-
- [1] R. Albert, A.L. Barabási, Rev. Mod. Phys. **74**, 47 (2002).
[2] S. N. Dorogovtsev, A. V. Goltsev, and J. F. F. Mendes, Rev. Mod. Phys. **80**, 1275 (2008).
[3] M. Barthélemy, A. Barrat, and A. Vespignani, *Dynamical processes on complex networks*, (Cambridge Univ. Press, Cambridge 2008).
[4] R. Pastor-Satorras and A. Vespignani, *Evolution and Structure of the Internet: A Statistical Physics Approach*, Cambridge University Press, Cambridge (2004).
[5] R. B. Griffiths, Phys. Rev. Lett. **23**, 17 (1969); B. M. McCoy, Phys. Rev. Lett. **23**, 383 (1969).
[6] A. J. Bray, Phys. Rev. Lett. **59**, 586 (1987). D. Dhar, M. Randeira, and J. P. Sethna, Europhys. Lett. **5**, 485 (1988). H. Rieger and A. P. Young, Phys. Rev. B **54**, 3328 (1996). D. S. Fisher, Phys. Rev. Lett. **69**, 534 (1992).
[7] A. J. Noest, Phys. Rev. Lett. **57**, 91 (1986). A. J. Noest, Phys. Rev. B **38**, 2715 (1988). R. Cafiero, A. Gabrielli and M.A. Muñoz, Phys. Rev. E. **57**, 5060 (1998).
[8] T. Vojta, J. Phys. A: Math. Gen. **39**, R143 (2006).
[9] G. Caldarelli, A. Capocci, P. De Los Rios, M. A. Muñoz, Phys. Rev. Lett. **89**, 258702 (2002).
[10] T. E. Harris, Ann. Prob., **2**, 969 (1974).

- [11] P. Erdős, A. Rényi, *Publicationes Mathematicae* **6**, 290 (1959).
- [12] M. A. Muñoz, R. Juhász, C. Castellano, and G. Ódor, *Phys. Rev. Lett.* **105**, 128701 (2010).
- [13] M. Henkel, H. Hinrichsen, and S. Lübeck, *Nonequilibrium Phase transitions* (Springer, Berlin 2008).
- [14] C. Castellano and R. Pastor-Satorras, *Phys. Rev. Lett.* **96**, 038701 (2006).
- [15] B. Bollobás, *Random Graphs*, Cambridge Studies in Adv. Math. **73**. Cambridge University Press, Cambridge, 2001.
- [16] R. Cohen, K. Erez, D. ben-Avraham, and S. Havlin, *Phys. Rev. Lett.* **85**, 4626 (2000).
- [17] M.Y. Lee and T. Vojta, *Phys. Rev. E* **79**, 041112 (2009).
- [18] J. Marro and R. Dickman, *Non-equilibrium phase transitions in lattice models*, Cambridge Univ. Press, (Cambridge 2005).
- [19] G. Ódor, *Universality in Nonequilibrium Lattice Systems*, World Scientific, 2008; *Rev. Mod. Phys.* **76**, 663 (2004).
- [20] A. J. Bray and G. J. Rodgers, *Phys. Rev. B* **38**, 11461 (1988). M. E. J. Newman, S. H. Strogatz, and D. J. Watts, *Phys. Rev. E* **64**, 026118 (2001).
- [21] I.A. Kovács and F. Iglói, *Phys. Rev. B* **83**, 174207 (2011). See also, I.A. Kovács and F. Iglói, *J. Phys.: Condens. Matter* **23**, 404204 (2011).
- [22] V. M. Eguíluz and K. Klemm, *Phys. Rev. Lett.* **89**, 108701 (2002). A. Vázquez and Y. Moreno, *Phys. Rev. E* **67**, 015101(R) (2003).
- [23] M. Catanzaro, M. Boguñá, and R. Pastor-Satorras, *Phys. Rev. E* **71**, 027103 (2005).
- [24] See M.M. de Oliveira, S.G. Alves, S.C. Ferreira, and R. Dickman, *Phys. Rev. E* **78** 031133 (2008), and refs. therein.
- [25] M. Aizenman and C.M. Newman, *Commun. Math. Phys.* **107**, 611 (1986).
- [26] M.E.J. Newman and D.J. Watts, *Phys. Lett. A* **263**, 341 (1999).
- [27] I. Benjamini and N. Berger, *Rand. Struct. Alg.* **19**, 102 (2001).
- [28] P. Sen and B. Chakrabarti, *J. Phys. A: Math. Gen.* **34**, 7749 (2001).
- [29] C.F. Moukarzel and M. Argollo de Menezes, *Phys. Rev. E* **65**, 056709 (2002).
- [30] D. Coppersmith, D. Gamarnik and M. Sviridenko, *Rand. Struct. Alg.* **21**, 1 (2002).
- [31] J.M. Kleinberg, *Nature* **406**, 845 (2000).
- [32] R. Juhász, G. Ódor, *Phys. Rev. E* **80**, 041123 (2009).
- [33] R. Juhász, *Phys. Rev. E* **78**, 066106 (2008).
- [34] M. Biskup, *Rand. Struct. Alg.* (2010)
- [35] R. Juhász, preprint, arXiv:1110.4222
- [36] J. Hooyberghs, F. Iglói, and C. Vanderzande, *Phys. Rev. Lett.* **90**, 100601 (2003); *Phys. Rev. E* **69**, 066140 (2004).
- [37] J. A. Hoyos, *Phys. Rev. E* **78**, 032101 (2008).
- [38] T. Vojta, A. Farquhar, J. Mast, *Phys. Rev. E* **79**, 011111 (2009).
- [39] P. Grassberger and A. de la Torre, *Ann. Phys.* **122**, 373 (1979).
- [40] T. Vojta T and M. Dickison, *Phys. Rev. E* **72** (2005) 036126.
- [41] H. K. Janssen, *Phys. Rev. E* **55**, (1997) 6253.
- [42] D. Mollison, *J. R. Stat. Soc. B* **39**, (1977) 283.
- [43] H. Hinrichsen, *J. Stat. Mech.: Theor. Exp.* P07066 (2007).
- [44] H. K. Janssen, K. Oerding, F. van Wijland F and H. J. Hilhorst, *Eur. Phys. J. B* **7**, (1999) 137.
- [45] H. Hinrichsen and M. Howard, *Eur. Phys. J. B* **7**, (1999) 635.
- [46] S. Johnson, J. J. Torres, and J. Marro, *arXiv* : 1007.3122
- [47] X. Castelló, R. Toivonen, V. M. Eguíluz, J. Saramäki, K. Kaski and M. San Miguel, *EPL* **79** (2007) 66006.
- [48] A. Amir, Y. Oreg, and Y. Imry, *Phys. Rev. Lett.* **105**, 070601 (2010); *Phys. Rev. Lett.* **103**, 126403 (2009).